

Low gap amorphous GaN_{1-x}As_x alloys grown on glass substrate

K. M. Yu,^{1,a)} S. V. Novikov,² R. Broesler,^{1,3} Z. Liliental-Weber,¹ A. X. Levander,^{1,3}
V. M. Kao,¹ O. D. Dubon,^{1,3} J. Wu,^{1,3} W. Walukiewicz,¹ and C. T. Foxon²

¹Materials Sciences Division, Lawrence Berkeley National Laboratory, 1 Cyclotron Road, Berkeley, California 94720-8197, USA

²School of Physics and Astronomy, University of Nottingham, Nottingham NG7 2RD, United Kingdom

³Department of Materials Science & Engineering, University of California, Berkeley, California 94720, USA

(Received 29 July 2010; accepted 19 August 2010; published online 9 September 2010)

Amorphous GaN_{1-x}As_x layers with As content in the range of $x=0.1$ to 0.6 were grown by molecular beam epitaxy on Pyrex glass substrate. These alloys exhibit a wide range of band gap values from 2.2 to 1.3 eV. We found that the density of the amorphous films is ~ 0.8 – 0.85 of their corresponding crystalline value. These amorphous films have smooth morphology, homogeneous composition, and sharp well defined optical absorption edges. The measured band gap values for the crystalline and amorphous GaN_{1-x}As_x alloys are in excellent agreement with the predictions of the band anticrossing model. The high absorption coefficient of $\sim 10^5$ cm⁻¹ for the amorphous GaN_{1-x}As_x films suggests that relatively thin films (on the order of 1 μ m) are necessary for photovoltaic application. © 2010 American Institute of Physics. [doi:10.1063/1.3488826]

It is well established that dramatic restructuring of the electronic bands can be achieved by alloying the anions of a semiconductor with elements of very different electronegativity and/or size. These alloys—the so called highly mismatched alloys (HMAs) (Ref. 1) have electronic and optical properties very different from their original host materials. These unusual properties arise from the restructuring of the conduction (valence) band of the alloys due to the anticrossing interaction between localized impurity states and the extended conduction (valence) band states of the matrix, as described by the band anticrossing model (BAC).^{1,2} Typically only dilute HMAs (up to $\sim 10\%$) can be grown due to large miscibility gaps arising from the large differences in atomic size and electronegativity of the host and the alloying elements. Notable examples of dilute HMAs that have been explored in recent years include dilute As-rich²⁻⁵ and N-rich GaN_{1-x}As_x (Refs. 6–8) and dilute Te-rich ZnO_xTe_{1-x}.⁹

Recently, we overcame the miscibility gap of GaAs and GaN alloys using the low temperature molecular beam epitaxy (LT-MBE) growth method and synthesized GaN_{1-x}As_x alloys in the whole composition range on sapphire substrate.^{10,11} We found an increase in As content with decreasing growth temperature. The alloys are amorphous in the composition range of $0.17 < x < 0.75$ and crystalline outside this region. The amorphous films have smooth morphology, homogeneous composition and sharp, well defined optical absorption edges. The bandgap energy varies in a broad energy range from ~ 3.4 eV in GaN to ~ 0.8 eV at $x \sim 0.85$ and was found to be in excellent agreement with prediction of the BAC model.

The spectral range covered by the GaN_{1-x}As_x alloys provides an almost perfect fit to the solar spectrum offering the opportunity to design high efficiency multijunction solar cells using a single ternary alloy system. The amorphous nature of this alloy over a wide alloy range can also be advantageous since they can be deposited on low-cost glass substrate, further reducing the cost of such device. Recently

we have demonstrated the growth of GaN_{1-x}As_x alloys with a limited range of x on standard microscope glass slides at growth temperature below 250 °C.¹² In this paper we report the structural and optical properties GaN_{1-x}As_x alloys grown on Pyrex glass substrates by LT-MBE over a wide range of composition ($x=0.1$ to 0.6).

All GaNAs samples were grown on 2 in. Pyrex substrates by plasma-assisted MBE in a MOD-GENII system. The system has a HD-25 Oxford Applied Research RF activated plasma source to provide active nitrogen and elemental Ga is used as the group III-source. In all experiments we have used arsenic in the form of As₂ produced by a Veeco arsenic valved cracker. For the growth of all GaNAs samples, we have used the same active N flux with the total N beam equivalent pressure (BEP) $\sim 1.5 \times 10^{-5}$ Torr and the same deposition time (2 h) for the majority of the films. Since the Pyrex substrate is transparent, the growth temperature cannot be measured directly by a pyrometer. From the heater current we estimate the growth temperature to be in the range of 200 – 800 °C.

The composition and crystallinity of the films were measured by combined Rutherford backscattering spectrometry (RBS) and particle induced x-ray emission (PIXE) using a 2 MeV He ion beam and x-ray diffraction (XRD), respectively. The microstructure of the GaN_{1-x}As_x films was investigated using cross sectional transmission electron microscopy. A JEOL 3010 with 300 keV accelerating energy and a resolution of 2.4 Å, JEOL CM300 with sub-Angstrom resolution and a Philips Tecnai microscope for Z-contrast high resolution studies were used.

The band gaps of the films were measured using photo-modulated reflectance (PR) at room temperature. Radiation from a 300 W halogen tungsten lamp dispersed by a 0.5 m monochromator was focused on the samples as a probe beam. A chopped HeCd laser beam ($\lambda=442$ or 325 nm) provided the photomodulation. PR signals were detected by a Si or Ge photodiode using a phase-sensitive lock-in amplification system. The values of the band gap and the line width were determined by fitting the PR spectra with the Aspnes third-derivative functional form.¹³ The PR measured band

^{a)}Electronic mail: kmyu@lbl.gov.

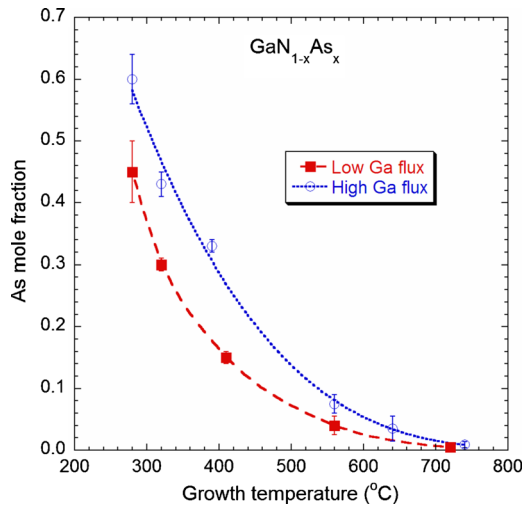


FIG. 1. (Color online) As mole fraction (x) in $\text{GaN}_{1-x}\text{As}_x$ films measured by RBS/PIXE as a function of growth temperature under high ($\text{BEP} \sim 1.1 \times 10^{-7}$ Torr) and low ($\text{BEP} \sim 7.1 \times 10^{-8}$ Torr) Ga flux condition.

gap of the GaNAs alloys is further confirmed by absorption spectroscopy using a LAMBDA-950 UV/Vis/NIR spectrophotometer over the range of 190–3300 nm.

Figure 1 shows the As mole fraction (x) in $\text{GaN}_{1-x}\text{As}_x$ films measured by RBS/PIXE as a function of growth temperature under high ($\text{BEP} \sim 1.1 \times 10^{-7}$ T) and low ($\text{BEP} \sim 7.1 \times 10^{-8}$ T) Ga flux condition, the dashed/dotted lines in the figure are quadratic fit of the data. As_2 flux in these growths was kept constant with $\text{BEP} \sim 7.2 \times 10^{-6}$ Torr. A monotonic increase in the As incorporation in the film is observed as the growth temperature is reduced. We found that $\text{GaN}_{1-x}\text{As}_x$ films have smooth morphology and uniform composition under lower Ga flux conditions. XRD measurements show that all films grown at temperatures lower than 500 °C are amorphous. While the $\text{GaN}_{1-x}\text{As}_x$ films are amorphous in the composition range of $0.17 < x < 0.75$ when grown on sapphire substrate,¹¹ for films grown on Pyrex substrates, the composition range for amorphous alloys extends to $x \sim 0.1$.

Figures 2(a) and 2(b) show the cross-sectional TEM micrographs for two $\text{GaN}_{1-x}\text{As}_x$ samples with $x=0.45$ and 0.15 . Both films show abrupt interfaces with the Pyrex substrate and a smooth surface. High resolution TEM micrographs [Figs. 2(f) and 2(g)] show “pepper and salt” contrast typical of amorphous structure without any local fringe images corresponding to the medium range structure. This contrast uniformity is observed starting from the interface to the sample surface indicating structural homogeneity of both samples. The amorphous nature of the films is also confirmed by selective area electron diffraction pattern (SAD) taken under parallel beam illumination [Figs. 2(c)–2(e)]. Halo rings are observed demonstrating that samples are amorphous. The diameter of the first halo rings in the SAD patterns from the two films are slightly different, with a smaller diameter for the sample with $x=0.45$ compared to the sample with $x=0.15$. This different in the halo ring diameter is consistent with the expected difference in the pair correlation function due to compositional change in the two samples. Moreover, a very weak intensity second ring is also observed for both these samples at higher scattering angles. A comparison of the areal densities measured by RBS and thickness values

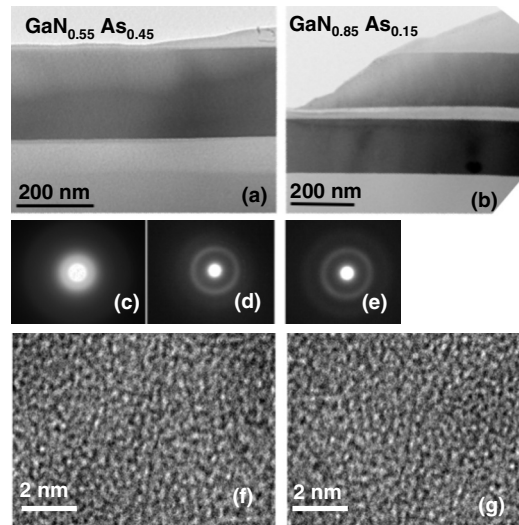


FIG. 2. Cross-sectional TEM micrographs and the SAD patterns for $\text{GaN}_{1-x}\text{As}_x$ samples: (a) $x=0.45$; (b) $x=0.15$; (c) SAD pattern from the Pyrex substrate; (d) SAD from the sample shown in (a); (e) SAD from the sample shown in (b); [(f) and (g)] high resolution images from respected samples indicating amorphous structure.

measured by TEM reveals that the density of the amorphous films is ~ 0.79 and 0.85 of their corresponding crystalline value (using Vegard’s law) for $\text{GaN}_{1-x}\text{As}_x$ films with $x=0.45$ and 0.15 , respectively.

The critical optical transitions of the $\text{GaN}_{1-x}\text{As}_x$ samples were measured using PR spectroscopy. Figure 3 shows a series of PR spectra from amorphous $\text{GaN}_{1-x}\text{As}_x$ samples with $x=0.15$ – 0.45 . A gradual decrease in the $\text{GaN}_{1-x}\text{As}_x$ band gap as x increases is clearly shown. These band gap values are further confirmed by optical absorption measurements that showed sharp absorption edges for all the amorphous films with absorption coefficient $\sim 1 \times 10^5 \text{ cm}^{-1}$ at ~ 0.5 eV above the band gap. The inset of Fig. 3 compares the PR and absorption spectra from a $\text{GaN}_{0.76}\text{As}_{0.24}$ sample. The clear observation of the PR signal indicates an extended

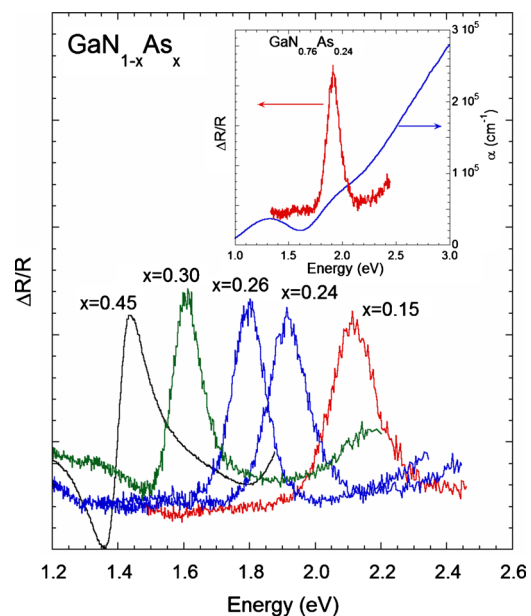


FIG. 3. (Color online) PR spectra from $\text{GaN}_{1-x}\text{As}_x$ thin films on pyrex substrate with x in the range of 0.15 – 0.45 . The inset shows a comparison between the PR and absorption spectra from a $\text{GaN}_{0.76}\text{As}_{0.24}$ sample.

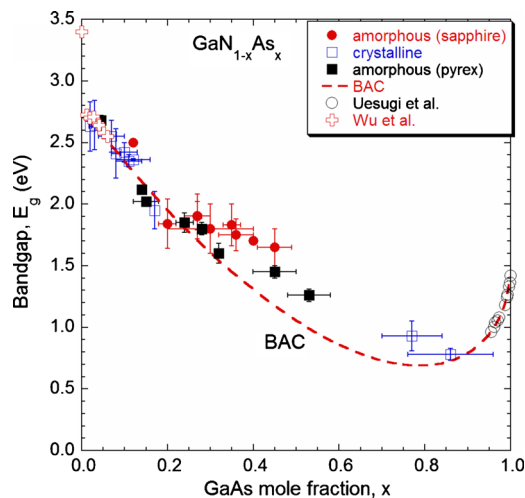


FIG. 4. (Color online) Band gap energy as a function of As content x for $\text{GaN}_{1-x}\text{As}_x$ alloys. Band gap values from both crystalline and amorphous alloys grown on sapphire and Pyrex are shown together with results from reported crystalline As-rich and N-rich $\text{GaN}_{1-x}\text{As}_x$ alloys (from Refs. 3 and 8). Calculated composition dependence of the band gap of $\text{GaN}_{1-x}\text{As}_x$ alloys based on the BAC is also shown.

rather than localized nature of the band edge states. This is also consistent with an abrupt onset of the absorption edges and an absence of defused absorption tails that are typical in amorphous silicon.

The band gap as measured by PR on the $\text{GaN}_{1-x}\text{As}_x$ films grown on Pyrex are shown in Fig. 4 together with data taken from films grown on sapphire. Band gap values for dilute alloys (As-rich³ and N-rich⁸ GaNAs) from the literature are also presented. The composition dependence of the band gap of $\text{GaN}_{1-x}\text{As}_x$ alloys over the entire composition range shown in Fig. 4 was calculated by a weighted interpolation of the BAC calculated curves for N-rich and As-rich dilute alloys.⁸ Our experimental band gap data (both on sapphire and Pyrex) for the crystalline and amorphous $\text{GaN}_{1-x}\text{As}_x$ alloys are in excellent agreement with the BAC model. Given the fact that the calculated band gap in BAC model is an interpolation of results from dilute crystalline GaNAs and GaAsN alloys, the agreement of the measured band gap for the amorphous alloys with the calculation is remarkable. The results suggest that for this composition range the amorphous $\text{GaN}_{1-x}\text{As}_x$ alloys have short-range ordering that resembles random crystalline $\text{GaN}_{1-x}\text{As}_x$ alloys.

We have demonstrated the possibility of growing amorphous $\text{GaN}_{1-x}\text{As}_x$ films with variable As content on glass

substrates. The large band gap range of the amorphous phase of GaNAs covers much of the solar spectrum and therefore this material system is a good candidate for full spectrum multijunction solar cells. The amorphous nature of the GaNAs alloys is particularly advantageous since no lattice matching is required and low cost substrates such as glass can be used for solar cell fabrication. The high absorption coefficient of $\sim 10^5 \text{ cm}^{-1}$ for the amorphous $\text{GaN}_{1-x}\text{As}_x$ films suggests that relatively thin films (on the order of $1 \mu\text{m}$) are necessary for photovoltaic application. This further reduces the cost of solar cells fabricated using this material.

This work was supported by the Director, Office of Science, Office of Basic Energy Sciences, Materials Sciences and Engineering Division, of the U.S. Department of Energy under Contract No. DE-AC02-05CH11231. The work at the University of Nottingham was undertaken with support from the EPSRC (Grant Nos. EP/G046867/1, EP/G030634/1, and EP/I004203/1).

- ¹W. Walukiewicz, W. Shan, K. M. Yu, J. W. Ager III, E. E. Haller, I. Miotkowski, M. J. Seong, H. Alawadhi, and A. K. Ramdas, *Phys. Rev. Lett.* **85**, 1552 (2000).
- ²W. Shan, W. Walukiewicz, J. W. Ager III, E. E. Haller, J. F. Geisz, D. J. Friedman, J. M. Olson, and S. R. Kurtz, *Phys. Rev. Lett.* **82**, 1221 (1999).
- ³K. Uesugi, N. Marooka, and I. Suemune, *Appl. Phys. Lett.* **74**, 1254 (1999).
- ⁴A. Erol, *Physics of Dilute III-V Nitride Semiconductors and Material Systems: Physics and Technology* (Springer, Berlin, 2008).
- ⁵W. Walukiewicz, K. Alberi, J. Wu, W. Shan, K. M. Yu, and J. W. Ager III, in *Physics of Dilute III-V Nitride Semiconductors and Material Systems: Physics and Technology*, edited by A. Erol (Springer, Berlin, 2008), Chap. 3.
- ⁶C. T. Foxon, I. Harrison, S. V. Novikov, A. J. Winsor, R. P. Campion, and T. Li, *J. Phys.: Condens. Matter* **14**, 3383 (2002).
- ⁷A. Kimura, C. A. Paulson, H. F. Tang, and T. F. Kuech, *Appl. Phys. Lett.* **84**, 1489 (2004).
- ⁸J. Wu, W. Walukiewicz, K. M. Yu, J. D. Denlinger, W. Shan, J. W. Ager, A. Kimura, H. F. Tang, and T. F. Kuech, *Phys. Rev. B* **70**, 115214 (2004).
- ⁹K. M. Yu, W. Walukiewicz, J. Wu, W. Shan, J. W. Beeman, M. A. Scarpulla, O. D. Dubon, and P. Becla, *Phys. Rev. Lett.* **91**, 246403 (2003).
- ¹⁰S. V. Novikov, C. R. Staddon, A. V. Akimov, R. P. Campion, N. Zainal, A. J. Kent, C. T. Foxon, C.-H. Chen, K. M. Yu, and W. Walukiewicz, *J. Cryst. Growth* **311**, 3417 (2009).
- ¹¹K. M. Yu, S. V. Novikov, R. Broesler, I. N. Demchenko, J. D. Denlinger, Z. Liliental-Weber, F. Luckert, R. W. Martin, W. Walukiewicz, and C. T. Foxon, *J. Appl. Phys.* **106**, 103709 (2009).
- ¹²S. V. Novikov, C. R. Staddon, C. T. Foxon, K. M. Yu, R. Broesler, M. Hawkrigde, Z. Liliental-Weber, W. Walukiewicz, J. Denlinger, and I. Demchenko, *J. Vac. Sci. Technol. B* **28**, C3B12 (2010).
- ¹³D. E. Aspnes, *Surf. Sci.* **37**, 418 (1973).